Article

Weak Intramolecular Interactions in Ethylene Glycol Identified by Vapor Phase OH–Stretching Overtone Spectroscopy

Daryl L. Howard, Poul Jrgensen, and Henrik G. Kjaergaard

J. Am. Chem. Soc., **2005**, 127 (48), 17096-17103• DOI: 10.1021/ja055827d • Publication Date (Web): 11 November 2005

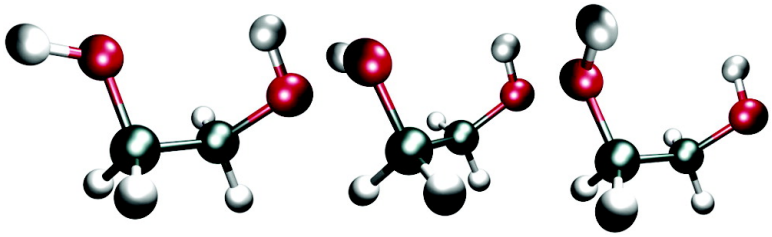

J|A|C|S
ARTICLES
Published on Web 11/11/2005

Weak Intramolecular Interactions in Ethylene Glycol Identified by Vapor Phase OH−Stretching Overtone Spectroscopy

Daryl L. Howard,[†] Poul Jørgensen,[‡] and Henrik G. Kjaergaard*,[†]

Contribution from the Department of Chemistry, University of Otago, P. O. Box 56, Dunedin, New Zealand, and Department of Chemistry, Aarhus University, DK-8000 Århus C, Denmark

Received August 25, 2005; E-mail: henrik@alkali.otago.ac.nz

Abstract: Vapor phase OH-stretching overtone spectra of ethylene glycol were recorded to investigate weak intramolecular hydrogen bonding. The spectra were recorded with conventional absorption spectroscopy and laser photoacoustic spectroscopy in the first to fourth OH-stretching overtone regions. The room-temperature spectra are dominated by two conformers that show weak intramolecular hydrogen bonding. A less abundant third conformer, with no sign of hydrogen bonding, is also observed. Vapor phase spectra of the ethylene-d_4 glycol isotopomer were also recorded and used to identify an interfering resonance between CH-stretching and OH-stretching states in the fourth overtone. Anharmonic oscillator local mode calculations of the OH-stretching transitions have provided an accurate simulation of the observed spectra. The local mode parameters were calculated with coupled cluster ab initio methods. The calculations facilitate assignment of the different conformers in the spectra and illustrate the effect of the intramolecular hydrogen bonding.

Introduction

Ethylene glycol (EG), or 1,2-ethanediol, is one of the simplest molecules with two vicinal hydroxyl groups, and as such, it can serve as a simple model for biological molecules such as sugars and as a prototype for intramolecular hydrogen bonding. In EG, the intramolecular hydrogen bond conformation is comprised of a five-membered quasi-ring. The hydrogen bond angle in a five-membered ring is far from an optimal linear conformation,[1] and the intramolecular hydrogen bond is expected to be weak. EG is a triple rotor molecule that can exist in one of $3^3 = 27$ conformations. Some of the structures are degenerate due to symmetry, and the number of unique conformations is reduced to 10. The 10 conformers are shown in Figure 1 along with their structural degeneracies. The conformers are specified according to the three dihedral angles about each of the two C−O bonds and about the C−C bond, and the nomenclature as described by Cramer and Truhlar has been used.[2]

There have been numerous theoretical calculations on EG ranging from Hartree−Fock, MP2, B3LYP, and QCISD levels of theory. The general finding from the calculations have indicated that the two lowest energy conformers (**1** and **2** in Figure 1) contain a weak intramolecular hydrogen bond configuration.[3−18] There have been infrared,[19] electron diffraction,[20,21] and microwave[22−27] gas-phase studies of EG. The rotation-tunneling spectrum recorded in the millimeter and submillimeter regions has also been recorded in the gas phase.[28,29] These studies have focused primarily on the lowest

[†] University of Otago.
[‡] Aarhus University.

(1) Pimentel, G. C.; McClellan, A. L. *The Hydrogen Bond*; W. H. Freeman: San Francisco, 1960.
(2) Cramer, C. J.; Truhlar, D. G. *J. Am. Chem. Soc.* **1994**, *116*, 3892−3900.
(3) Radom, L.; Lathan, W. A.; Hehre, W. J.; Pople, J. A. *J. Am. Chem. Soc.* **1973**, *95*, 693−698.
(4) Van Alsenoy, C.; Van Den Enden, L. *J. Mol. Struct. (THEOCHEM)* **1984**, *108*, 121−128.
(5) Nagy, P. I.; Dunn, W. J., III; Alagona, G.; Ghio, C. *J. Am. Chem. Soc.* **1991**, *113*, 6719−6729.
(6) Nagy, P. I.; Dunn, W. J., III; Alagona, G.; Ghio, C. *J. Am. Chem. Soc.* **1992**, *114*, 4752−4758.
(7) Murcko, M. A.; DiPaola, R. A. *J. Am. Chem. Soc.* **1992**, *114*, 10010−10018.
(8) Carmichael, I.; Chipman, D. M.; Podlasek, C. A.; Serianni, A. S. *J. Am. Chem. Soc.* **1993**, *115*, 10863−10870.
(9) Oie, T.; Topol, I. A.; Burt, S. K. *J. Phys. Chem.* **1994**, *98*, 1121−1128.
(10) Yeh, T.-S.; Chang, Y.-P.; Su, T.-M. *J. Phys. Chem.* **1994**, *98*, 8921−8929.
(11) Teppen, B. J.; Cao, M.; Frey, R. F.; van Alsenoy, C.; Miller, D. M.; Schäfer, L. *J. Mol. Struct. (THEOCHEM)* **1994**, *314*, 169−190.
(12) Csonka, G. I.; Anh, N.; Ángyán, J.; Csimadia, I. G. *Chem. Phys. Lett.* **1995**, *245*, 129−135.
(13) Reiling, S.; Brickmann, J.; Schlenkrich, M.; Bopp, P. A. *J. Comput. Chem.* **1996**, *17*, 133−147.
(14) Chang, Y.-P.; Su, T.-M.; Li, T.-W.; Chao, I. *J. Phys. Chem. A* **1997**, *101*, 6107−6117.
(15) Klein, R. A. *J. Comput. Chem.* **2002**, *23*, 585−599.
(16) Trindle, C.; Crum, P.; Douglass, K. *J. Phys. Chem. A* **2003**, *107*, 6236−6242.
(17) Mandado, M.; Graña, A. M.; Mosquera, R. A. *Phys. Chem. Chem. Phys.* **2004**, *6*, 4391−4396.
(18) Crittenden, D. L.; Thompson, K. C.; Jordan, M. J. T. *J. Phys. Chem. A* **2005**, *109*, 2971−2977.
(19) Buckley, P.; Giguère, P. A. *Can. J. Chem.* **1967**, *45*, 397−407.
(20) Bastiansen, O. *Acta Chem. Scand.* **1949**, *3*, 415−421.
(21) Kazerouni, M. R.; Hedberg, L.; Hedberg, K. *J. Am. Chem. Soc.* **1997**, *119*, 8324−8331.
(22) Marstokk, K. M.; Møllendal, H. *J. Mol. Struct.* **1974**, *22*, 301−3.
(23) Walder, E.; Bauder, A.; Günthard, H. H. *Chem. Phys.* **1980**, *51*, 223−239.
(24) Caminati, W.; Corbelli, G. *J. Mol. Spectrosc.* **1981**, *90*, 572−578.
(25) Kristiansen, P.-E.; Marstokk, K.-M.; Møllendal, H. *Acta Chem. Scand. A* **1987**, *41*, 403−414.
(26) Christen, D.; Coudert, L. H.; Suenram, R. D.; Lovas, F. J. *J. Mol. Spectrosc.* **1995**, *172*, 57−77.
(27) Christen, D.; Coudert, L. H.; Larsson, J. A.; Cremer, D. *J. Mol. Spectrosc.* **2001**, *205*, 185−196.
(28) Christen, D.; Müller, H. S. P. *Phys. Chem. Chem. Phys.* **2003**, *5*, 3600−3605.

10.1021/ja055827d CCC: $30.25

energy conformer; however, the second most stable EG conformer has been identified in rotational spectra.[25,27,29] In the infrared spectrum, two peaks separated by 33 cm^{-1} were observed in the OH-streching region and attributed to the free and hydrogen bonded OH-stretching transitions.[19] Due to the congestion in the infrared spectrum, no specific conformer could be identified. To complement the infrared gas phase study, several low-temperature matrix isolation studies have been performed.[30−32] The matrix spectra are complicated by the large matrix frequency shifts, the possibility of different sites and irreversible changes due to the irradiation by infrared light.[30] However, the two lowest energy conformers have been identified.[30,32] Recently, there has been spectroscopic detection of EG in interstellar space[33] and in comet Hale-Bopp.[34]

Recently, the existence of an intramolecular hydrogen bonding in EG has been questioned. Theoretical studies by Klein[15] and Mandado et al.[17] have concluded that an intramolecular hydrogen bond is not present in EG based on the hydrogen bonding criteria suggested by Koch and Popelier.[35] However, no standard criteria have yet been established for characterizing the presence and strength of intramolecular hydrogen bonds. Infrared spectroscopy is the classical experimental method for identifying hydrogen bonds. For a hydroxyl group, the intensity increase and the wavenumber redshift of the OH-stretching fundamental transition are considered to be a spectroscopic signature of a hydrogen bond, and the magnitude of each increases with increasing hydrogen bond strength.[1,36,37] Conversely, the intensity of the first OH-stretching overtone is weaker than usual upon hydrogen bonding[38] and the redshift is approximately double that observed in the fundamental.[1,39] For several years, the "disappearance" of the first overtone was used as a criterion for strong hydrogen bonding.[1] However, there is little vibrational overtone data of hydrogen bonding in the gas phase. There are two main reasons for this. The first is that overtone transitions are inherently weak, and their intensity typically drops by an order of magnitude with each quantum of vibrational excitation. The second is that many species that undergo hydrogen bonding have relatively low vapor pressures.[1] Thus, one or a combination of conditions such as long sample path lengths, high temperatures, or sensitive spectroscopic techniques are required to overcome these hurdles. Our goal is to observe the role, if any, of intramolecular hydrogen bonding in EG through the analysis of its vapor phase OH-stretching overtone spectrum.

Overtone spectra of XH-stretching vibrations (X is any heavy atom) are very sensitive to bond properties, and they can be used to study subtle effects in molecular structure and molecular conformation.[40] Anharmonic oscillator local mode calculations have been successful in the calculation of XH-stretching overtone spectra[41,42] and in studies of weak intramolecular interactions.[43,44]

We have performed a statistical thermodynamics population analysis of the 10 conformers of EG at the B3LYP/aug-cc-pVTZ level. Geometry optimizations were subsequently performed at the coupled cluster singles and doubles with perturbative triples (CCSD(T))[45] level on the three lowest energy conformers. Local mode theory was used to calculate the OH-stretching spectra for the three conformers considered to dominate the room-temperature vibrational spectra. The required local mode frequencies and anharmonicities of the OH-stretching modes as well as the dipole moment functions were calculated at the CCSD(T) level.

The vapor phase spectra of EG and of the ethylene-d_4 glycol isotopomer ($HOCD_2CD_2OH$, EG-d_4) have been recorded up to the fourth OH-stretching overtone. The spectra of the EG-d_4 glycol was recorded to eliminate an interfering resonance with an OH- and CH-stretching combination state.

Experimental Section

The samples of ethylene glycol ($HOCH_2CH_2OH$, Unilab, LR Grade) and ethylene-d_4 glycol ($HOCD_2CD_2OH$, Aldrich, 98% atom D) were not further purified except for degassing and drying as described below.

The $\Delta\nu_{OH} = 2$ region of EG vapor was recorded with a Cary 500 spectrometer and a 4.8 m path length cell (Infrared Analysis) at room temperature. The sample was placed in a flask on a vacuum line and degassed by several freeze−pump−thaw cycles, and subsequently pumped on the vacuum line for an hour to help remove H_2O. The vacuum line was then closed and the vapor was allowed to equilibrate throughout the vacuum line and the cell.

The $\Delta\nu_{OH} = 3-5$ regions of EG vapor were recorded with intracavity laser photoacoustic spectroscopy. Our photoacoustic spectrometer has been described previously.[47] Briefly, a Coherent Innova Sabre argon ion laser running at all lines was used to pump a Coherent 890 titanium: sapphire laser to record the $\Delta\nu_{OH} = 3$ and 4 regions and a Coherent 599 dye laser with R6G dye to record the $\Delta\nu_{OH} = 5$ region. The bandwidth of the tunable lasers is approximately 1 cm^{-1}. The photoacoustic cell contained a Knowles EK3133 microphone for detection of the photoacoustic signal.

Sample preparation for the photoacoustic spectra was as follows. About 0.1 mL of EG was transferred directly into the sample arm of the photoacoustic cell and degassed on a vacuum line with several freeze−pump−thaw cycles. Due to the low vapor pressure of EG, approximately 0.05 Torr at 20 °C, it was necessary to dry the sample very well to prevent the spectra being swamped by H_2O transitions. To remove as much H_2O as possible, the cell and sample were evacuated on a vacuum line for about 4 h until approximately 10% of the original sample volume remained in the sample arm. Nevertheless absorption by H_2O vapor was interfering in the high wavenumber portion of the $\Delta\nu_{OH} = 5$ region, and a spectrum of H_2O vapor was recorded and spectrally subtracted from the EG spectrum. To enhance the photoacoustic signal, a buffer gas of 200 Torr argon was added to the photoacoustic cell for all the spectra.[48,49]

(29) Müller, H. S. P.; Christen, D. *J. Mol. Spectrosc.* **2004**, *228*, 298−307.
(30) Frei, H.; Ha, T.-K.; Meyer, R.; Günthard, H. H. *Chem. Phys.* **1977**, *25*, 271−298.
(31) Coleman, W. M., III; Gordon, B. M. *Appl. Spectrosc.* **1988**, *42*, 671−674.
(32) Park, C. G.; Tasumi, M. *J. Phys. Chem.* **1991**, *95*, 2757−2762.
(33) Hollis, J. M.; Lovas, F. J.; Jewell, P. R.; Coudert, L. H. *Astrophys. J.* **2002**, *571*, L59−L62.
(34) Crovisier, J., J.; Bockelée-Morvan, D.; Biver, N.; Colom, P.; Despois, D.; Lis, D. C. *Astron. Astrophys.* **2004**, *418*, L35−L38.
(35) Koch, U.; Popelier, P. L. A. *J. Phys. Chem.* **1995**, *99*, 9747−9754.
(36) Iogansen, A. V. *Spectrochim. Acta Part A* **1999**, *55*, 1585−1612.
(37) Del Bene, J. E.; Jordan, M. J. T. *Int. Rev. Phys. Chem.* **1999**, *18*, 119−162.
(38) Hilbert, G. E.; Wulf, O. R.; Hendricks, S. B.; Liddel, U. *J. Am. Chem. Soc.* **1936**, *58*, 548−555.
(39) Sandorfy, C. *Top. Curr. Chem.* **1984**, *120*, 41−84.
(40) Henry, B. R. *Acc. Chem. Res.* **1987**, *20*, 429−435.
(41) Kjaergaard, H. G.; Yu, H.; Schattka, B. J.; Henry, B. R.; Tarr, A. W. *J. Chem. Phys.* **1990**, *93*, 6239−6248.
(42) Howard, D. L.; Kjaergaard, H. G. *J. Chem. Phys.* **2004**, *121*, 136−140.
(43) Kjaergaard, H. G.; Howard, D. L.; Schofield, D. P.; Robinson, T. W.; Ishiuchi, S.; Fujii, M. *J. Phys. Chem. A* **2002**, *106*, 258−266.
(44) Robinson, T. W.; Kjaergaard, H. G.; Ishiuchi, S.; Shinozaki, M.; Fujii, M. *J. Phys. Chem. A* **2004**, *108*, 4420−4427.
(45) Raghavachari, K.; Trucks, G. W.; Pople, J. A.; Head-Gordon, M. *Chem. Phys. Lett.* **1989**, *157*, 479−483.
(46) Helgaker, T.; Ruden, T. A.; Jørgensen, P.; Olsen, J.; Klopper, W. *J. Phys. Org. Chem.* **2004**, *17*, 913−933.
(47) Rong, Z.; Kjaergaard, H. G. *J. Phys. Chem. A* **2002**, *106*, 6242−6253.
(48) Wake, D. R.; Amer, N. M. *Appl. Phys. Lett.* **1979**, *34*, 379−381.

Variable temperature photoacoustic experiments were conducted with a 250 W heat lamp that was suspended over the cell. The temperature was varied by altering the distance of the lamp to the cell. The cavity of the laser where the photoacoustic cell is placed was lined with aluminum foil to reflect heat. Due to the limitations of our photoacoustic cell, the temperature was kept below 60 °C. It took about 15 min for the temperature to equilibrate. The temperature was measured with the probe of a digital thermometer placed next to the microphone of the photoacoustic cell, and remained within ± 1 °C during a scan.

Vibrational Theory. The vibrations of OH-stretching oscillators are anharmonic, and their highly excited vibrations are generally best described by a local mode model.[50,51] We have used an anharmonic oscillator local mode model to characterize the OH-stretching modes. The Hamiltonian is approximated as a Morse oscillator

$$[H^\circ - E^\circ_{|0\rangle}]/hc = v\tilde{\omega} - (v^2 + v)\tilde{\omega}x \quad (1)$$

where h is Planck's constant, c is the speed of light, $E^\circ_{|0\rangle}$ is the zero order energy of the vibrational ground state, v is the vibrational quantum number, and $\tilde{\omega}$ and $\tilde{\omega}x$ are the local mode frequency and anharmonicity, respectively. This leads to the well-known two-parameter Morse oscillator energy expression

$$\tilde{\nu}/v = \tilde{\omega} - (v + 1)\tilde{\omega}x \quad (2)$$

where $\tilde{\nu}$ is the transition energy in cm^{-1} from $v = 0$ to v, from which $\tilde{\omega}$ and $\tilde{\omega}x$ can be obtained.

The dimensionless oscillator strength f of a vibrational transition from the ground state g to an excited state e is given by[41,52]

$$f = 4.702 \times 10^{-7}[\text{cm D}^{-2}]\tilde{\nu}_{eg}\,|\vec{\mu}_{eg}|^2 \quad (3)$$

where $\tilde{\nu}_{eg}$ is the transition energy in cm^{-1} and $\vec{\mu}_{eg} = \langle e|\vec{\mu}|g\rangle$ is the transition dipole moment in debye (D).

The dipole moment function is approximated by a series expansion in the internal displacement coordinate q about the equilibrium geometry

$$\vec{\mu}(q) = \sum_i \vec{\mu}_i q^i \quad (4)$$

where the coefficients $\vec{\mu}_i$ are given by

$$\vec{\mu}_i = \frac{1}{i!}\frac{\partial^i \vec{\mu}}{\partial q^i}\bigg|_e \quad (5)$$

The coefficients $\vec{\mu}_i$ are determined from an ab initio calculated one-dimensional grid of the dipole moment $\vec{\mu}(q)$. The grid points are calculated by serially displacing q by ± 0.2 Å from equilibrium in steps of 0.05 Å for a total of nine points. We have limited the series expansion of the dipole moment to fifth order.[42,53]

The OH-stretching frequency and anharmonicity are obtained from the second (f_{ii}), third (f_{iii}) and fourth (f_{iv}) order derivatives of the potential energy with respect to the OH-stretching coordinate according to[54,55]

$$\tilde{\omega} = \frac{\sqrt{f_{ii}G_{ii}}}{2\pi c} \quad (6)$$

$$\tilde{\omega}x = \frac{hG_{ii}}{64\pi^2 c f_{ii}}\left(\frac{5f_{iii}^{\,2}}{3f_{ii}} - f_{iv}\right) \quad (7)$$

where G_{ii} is the reciprocal of the OH reduced mass. Previously we have obtained $\tilde{\omega}x$ by using the expression derived by Sowa et al.,[56] which depends only on the second- and third-order derivatives of the energy.[53] We have found that use of eq 7 gives $\tilde{\omega}x$ values that are in significantly better agreement with experimental observations for H_2O.[54]

Results and Discussion

Population Analysis. The purpose of the theoretical population analysis is to predict which conformers that contribute to the vibrational spectra at a given temperature. Standard statistical mechanical relationships[57,58] were used to calculate the free energies and thus the relative populations of the 10 EG conformers in a manner similar to that performed by Cramer and Truhlar.[2] The population analysis was calculated at the B3LYP/aug-cc-pVTZ level in Gaussian03.[59] The calculated relative electronic energies ΔE, the relative zero point vibrational energy (ZPVE) corrected energies ΔE_0 and the relative free energies ΔG of the conformers are presented in Table 1. Each unique conformer has a contribution to its free energy of $-RT\ln\Omega$, where Ω is the structural degeneracy of the conformer as listed in Figure 1. This degeneracy contribution to the free energy is included in the ΔG values in Table 1. The fractional gas-phase equilibrium populations F(M) of a conformer M were calculated according to a Boltzmann distribution scheme[2]

$$F(M) = \frac{\exp(-G^\circ_M/RT)}{\sum_i \exp(-G^\circ_i/RT)} \quad (8)$$

where i spans all 10 unique conformers. We have used the ΔG values from Table 1 for G°_M and G°_i in eq 8. Conformers tG^+g^- (58%), $g^+G^+g^-$ (26%) and $g^-G^+g^-$ (10%), hereafter referred to as **1**, **2**, and **3**, respectively, are calculated to comprise the majority of the EG population at 298 K. The remaining conformers are calculated to have negligible populations at room temperature. Our results are in agreement with those of Cramer and Truhlar.[2] The largest discrepancy is for **3**, for which Cramer and Truhlar obtained 13% compared to 10% obtained in this study. The fully trans conformer *tTt* is noteworthy since it is calculated to be the fourth most stable structure with respect to electronic energy and zero point energy, however its structural degeneracy of unity significantly "increases" its free energy relative to the more degenerate conformers.

The three lowest energy conformers are all gauche (designated G^+) with respect to the C−C torsion. This is in agreement with a prediction based on the gauche effect,[60] which is a tendency for a molecule to adopt a structure that has the maximum number of gauche interactions between the adjacent electron pairs and/or polar bonds.

(49) Schattka, B. J.; Turnbull, D. M.; Kjaergaard, H. G.; Henry, B. R. *J. Phys. Chem.* **1995**, *99*, 6327−6332.
(50) Henry, B. R. *Acc. Chem. Res.* **1977**, *10*, 207−213.
(51) Jensen, P. *Mol. Phys.* **2000**, *98*, 1253−1285.
(52) Atkins, P. W.; Friedman, R. S. *Molecular Quantum Mechanics*, 3rd ed.; Oxford University Press: Oxford, 1997.
(53) Low, G. R.; Kjaergaard, H. G. *J. Chem. Phys.* **1999**, *110*, 9104−9115.
(54) Kjaergaard, H. G., Unpublished work.
(55) Herzberg, G. *Spectra of Diatomic Molecules*, 2nd ed.; D. Van Nostrand: New York, 1950.
(56) Sowa, M. G.; Henry, B. R.; Mizugai, Y. *J. Phys. Chem.* **1991**, *95*, 7659−7664.
(57) McQuarrie, D. A. *Statistical Mechanics*; University Science Books: Sausalito, CA, 2000.
(58) Hehre, W. J.; Radom, L.; v. R. Schleyer, P.; Pople, J. A. *Ab Initio Molecular Orbital Theory*; Wiley: New York, 1986.
(59) Frisch, M. J.; et al. *Gaussian 03*, revision C.02; Gaussian, Inc.: Wallingford, CT, 2004.
(60) Wolfe, S. *Acc. Chem. Res.* **1972**, *5*, 102−111.

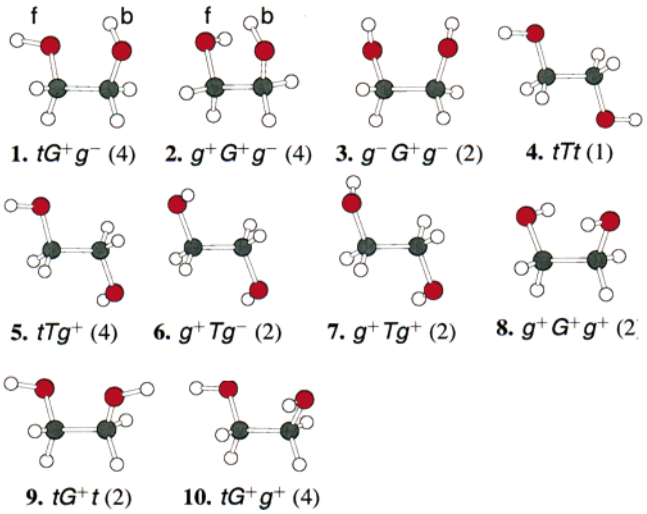

Figure 1. The 10 unique conformers of ethylene glycol. The structural degeneracy of each stereoisomer is indicated in parentheses. The free (f) and hydrogen bonded (b) OH bond is labeled in conformers **1** and **2**.

The conformers numbered **8** and **10** are somewhat deceptive looking as drawn in Figure 1 and appear to have an intramolecular hydrogen bond. However, the B3LYP/aug-cc-pVTZ calculated O−H···O distance is 0.6 and 0.9 Å longer for these two conformers, respectively, than the 2.4 Å distance calculated for **1** and **2**, and thus too large for effective hydrogen bonding to occur.[61]

CCSD(T) Geometry Optimizations. We have optimized the geometries of the three lowest energy conformers **1**, **2**, and **3** with the CCSD(T)[45] ab initio theory. The CCSD(T) theory is known to provide accurate molecular geometries and spectroscopic constants,[46] and we have utilized it in an attempt to avoid the empirical scaling of frequencies that is commonly performed in spectral simulations.[53] The computational cost of the CCSD(T) method is high, and the use of the desired aug-cc-pVTZ basis set was not feasible. To circumvent this problem, an approach was implemented in which both hydroxyl groups were modeled with the aug-cc-pVTZ basis set and the two methylene groups were modeled with the cc-pVTZ basis set. This was done in order to model the OH-stretching vibrations in the best possible manner while maintaining a good descriptive balance for the remainder of the molecule. We have labeled this composite basis set as aug′-cc-pVTZ. In a similar fashion we have used the smaller aug′-cc-pVDZ basis set, which we have compared to the aug-cc-pVDZ basis set. The CCSD(T) calculations were performed with MOLPRO.[62]

The CCSD(T)/aug′-cc-pVTZ calculated molecular parameters relating to the hydroxyl groups and the relative electronic energies for conformers **1**, **2**, and **3** are presented in Table 2. The labels used are as follows: rOH_b and rOH_f are the bonded and free OH bond lengths, respectively; $\Delta r_{OH} = rOH_b - rOH_f$; r_{HB} is the hydrogen bond length, defined as the distance between the acceptor oxygen atom and the donor hydrogen atom, and ∠HB is the hydrogen bond angle, i.e., the O−H···O angle. The OH_b bond length is calculated to be about 0.004 and 0.002 Å longer than OH_f in conformers **1** and **2**, respectively. A hydrogen bond length r_{HB} of approximately 2.33 Å is calculated for both conformers which is comparable to the 2.4 Å sum of the van der Waals radii of O (1.4 Å) and H (1.0 Å).[61,63] Since r_{HB} is not significantly less than 2.4 Å, the hydrogen bond interaction will be weak.[61,63] The hydrogen bond angles ∠HB of about 109° and 112° for **1** and **2** are far from the optimal linear configuration. For **3**, the calculated O−H···O distance of 2.7 Å is too large for effective hydrogen bonding to occur, and the O−H···O angle is highly unfavorable at 91°.

Table 1. Relative Energies (cm^{-1}) and Percentage Population at 298 K of the Ten Unique Ethylene Glycol Conformers

conformer	ΔE^a	$\Delta E_0{}^b$	ΔG^c	F(%)
1. tG^+g^-	0	0	0	57.7
2. $g^+G^+g^-$	120	146	167	25.7
3. $g^-G^+g^-$	283	219	355	10.4
4. tTt	821	699	1001	0.5
5. tTg^+	850	760	675	2.2
6. g^+Tg^-	840	770	854	0.9
7. g^+Tg^+	900	843	1086	0.3
8. $g^+G^+g^+$	944	776	888	0.8
9. tG^+t	970	782	895	0.8
10. tG^+g^+	1099	972	893	0.8

[a] Relative electronic energy (100 cm^{-1} = 1.196 kJ mol^{-1}). All energies calculated with the B3LYP/aug-cc-pVTZ method. [b] ZPVE corrected energy. [c] Free energy including degeneracy contribution.

Table 2. CCSD(T)/aug′-cc-pVTZ Optimized Geometric Parameters (Å and Degrees) and Relative Electronic Energies (cm^{-1}) of Ethylene Glycol

conformer	rOH_b	rOH_f	ΔrOH	r_{HB}	∠HB	ΔE
1	0.96440	0.96069	3.7×10^{-3}	2.33119	108.6	0
2	0.96519	0.96283	2.4×10^{-3}	2.32333	112.0	112
3		0.96193		2.70070	90.6	290

Observed Overtone Spectra. We have labeled the OH_b- and OH_f-stretching transitions of conformer **1** as **1**b and **1**f, respectively, and likewise for conformer **2**. Conformer **3** has two equivalent OH bonds due to its C_2 point group symmetry and is labeled **3**.

The observed vapor phase OH-stretching overtone spectrum of EG in the $\Delta v_{OH} = 2$ region is presented in Figure 2. The signal-to-noise ratio of the spectrum is low primarily due to the low sample pressure. The maximum absorbance of approximately 0.001 is at the detection limit of the Cary spectrometer. Since the quality of the spectrum in the $\Delta v_{OH} = 2$ region is poor, no quantitative information is derived from it.

(61) Schuster, P., Zundel, G., Sandorfy, C., Eds. *The Hydrogen Bond II. Structure and Spectroscopy*; North-Holland: Amsterdam, 1976.
(62) Werner, H.-J.; et al. Molpro, version 2002.6, a package of ab initio programs, 2003.
(63) Speakman, J. C. *The Hydrogen Bond and Other Intermolecular Forces*; The Chemical Society: London, 1975.

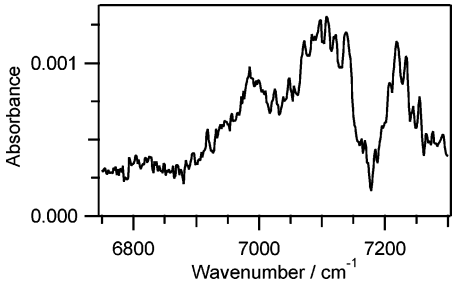

Figure 2. Vapor phase spectrum of ethylene glycol in the $\Delta v_{OH} = 2$ region recorded with a 4.8 m path length at 22 °C.

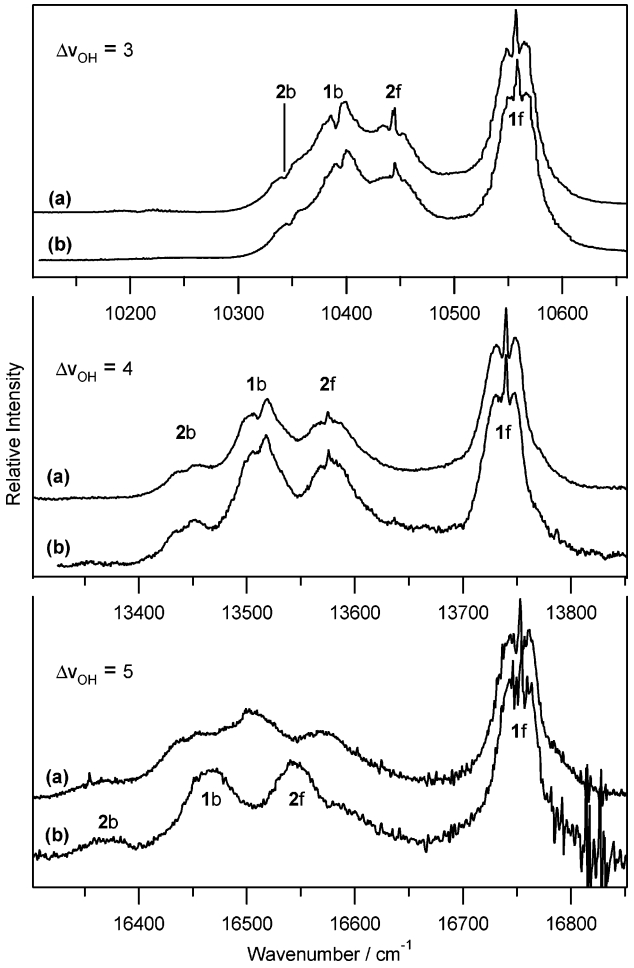

Figure 3. Vapor phase overtone spectra of (a) ethylene glycol and (b) ethylene-d_4 glycol in the $\Delta v_{OH} = 3-5$ regions recorded photoacoustically at 20 °C, 22 °C and 34 °C, respectively.

The band that lies above 7200 cm^{-1} is relatively narrow and is assigned to the **1**f transition. The band between 6900 and 7200 cm^{-1} is much broader and contains the transitions of **1**b, **2**b, **2**f and **3**.

The vapor phase OH-stretching overtone spectra of EG and EG-d_4 in the $\Delta v_{OH} = 3-5$ regions are presented in Figure 3. The abscissa of each overtone region is 550 cm^{-1} wide to illustrate the typical "spreading apart" of the transitions with increasing vibrational excitation. In these higher overtone spectra, it is possible to identify the transitions from the two lowest energy conformers, and the bonded and free transitions of **1** and **2** have been labeled. The band types observed for the OH-streching transitions of EG aid in the spectral assignments. Depending on how the transition moment is aligned along the lowest to highest moments of inertia (*a*, *b*, or *c* axis, respectively) for a particular vibration, a corresponding type A, B, or C rotational contour is observed. The **1**f and **2**f transitions give type A and C bands, respectively, which both have a central Q-branch; the **1**b and **2**b transitions produce type B bands which have a central minimum. The OH-stretching transitions of **3** yield a type B band, and the lack of a sharp Q-branch will make it more difficult to observe this minor conformer. Changes to the OH-stretching rotational contours are observed with increasing vibrational excitation. With the exception of the **1**f transition, the rotational contour of the OH-stretching transitions become less defined to the extent that the **2**b, **1**b and **2**f transitions of EG-d_4 have become featureless in the $\Delta v_{OH} = 5$ region. This trend indicates that the transition moment vector of these transitions is changing direction with increasing vibrational excitation, and this type of trend has been noted in formic acid, for example.[64] The observed wavenumbers of the transitions are listed in Table 3. These are determined from the location of the Q-branch, the dip in the peaks of the type *B* bands, and from spectral deconvolution of the EG-d_4 $\Delta v_{OH} = 5$ spectrum.

The spectra of both isotopomers in the $\Delta v_{OH} = 3$ and 4 regions are virtually identical and the observed transitions are within our estimated experimental uncertainty of ± 1 cm^{-1}. The vapor phase spectrum of EG in the $\Delta v_{OH} = 3$ region was reported by Badger and Bauer in 1936.[65] They observed two weak maxima with highly uncertain positions around 10 400 and 10 470 cm^{-1} in fair agreement with our spectra. In the $\Delta v_{OH} = 5$ region the spectra of the two isotopomers are significantly different. The EG-d_4 spectrum is consistent with the band profile of the lower overtones, whereas the EG spectrum is highly perturbed in the 16 400−16 600 cm^{-1} region due to resonance with OH-stretching and CH-stretching combination states (vide infra). Several spikes in the region around the **1**f transition in the $\Delta v_{OH} = 5$ spectra are residuals due to the imperfect spectral subtraction of H_2O vapor.

The **1**f transition is observed as the most intense band in the $\Delta v_{OH} = 3-5$ regions and it is well separated from the remaining three labeled transitions. The **2**b, **2**f, and **1**b transitions are within 100 cm^{-1} of each other at $\Delta v_{OH} = 3$, increasing to nearly 200 cm^{-1} at $\Delta v_{OH} = 5$. The **1**b transition is redshifted relative to the **1**f transition and likewise for **2**. At $\Delta v_{OH} = 5$, the redshifts are 285 and 173 cm^{-1} for **1** and **2**, respectively, which would suggest intramolecular hydrogen bonding in both conformers. However different environments of the hydroxyls can lead to substantial shifts as seen from the frequencies of the **1**f and **2**f transitions which are separated by 208 cm^{-1} at $\Delta v_{OH} = 5$, so the redshift within a conformer is not necessarily a measure of hydrogen bonding.

The observed local mode parameters, $\tilde{\omega}$ and $\tilde{\omega}x$, of the OH bonds in **1** and **2** are given in Tables 4 and 5. These were obtained from a fit of the observed OH-stretching transitions that are listed in Table 3 to eq 2. The small standard deviations obtained for the parameters are indicative of a good fit. The local mode frequencies of the OH_b-stretching vibrations are lower by 53 and 30 cm^{-1} than the corresponding OH_f transitions for conformers **1** and **2**, respectively. The anharmonicities of the OH_b-stretching vibrations are virtually identical to those of the OH_f bonds.

(64) Hurtmans, D.; Herregodts, F.; Herman, M.; Liévin, J.; Campargue, A.; Garnache, A.; Kachanov, A. A. *J. Chem. Phys.* **2000**, *113*, 1535−1545.
(65) Badger, R. M.; Bauer, S. H. *J. Chem. Phys.* **1936**, *4*, 711−715.

Table 3. Observed OH−Stretching Overtone Peak Positions (cm^{-1}) in Ethylene Glycol

Δv	**1**b	**1**f	**2**b	**2**f
3	10390	10557	10344	10444
4	13510	13740	13445	13575
5[a]	16466	16751	16370	16543

[a] The **1**b, **2**b, and **2**f transition wavenumbers were obtained from the ethylene-d_4 glycol spectrum.

Table 4. Observed and CCSD(T) Calculated OH−Stretching Local Mode Frequencies (cm^{-1})

basis set	**1**b	**1**f	**2**b	**2**f	**3**
cc-pVDZ	3801	3850	3784	3808	3827
aug′-cc-pVDZ	3786	3835	3772	3797	3814
aug-cc-pVDZ	3782	3829	3768	3794	3810
cc-pVTZ	3822	3873	3808	3837	3853
aug′-cc-pVTZ	3806	3856	3792	3823	3837
observed[a]	3803.3	3856.3	3796.1	3826.4	

[a] One standard deviation uncertainties are: ±2.2, ±0.9, ±0.7, ±3.6, respectively.

Table 5. Observed and CCSD(T) Calculated OH−Stretching Local Mode Anharmonicities (cm^{-1})

basis set	**1**b	**1**f	**2**b	**2**f	**3**
cc-pVDZ	86.5	88.4	87.5	89.0	88.3
aug′-cc-pVDZ	89.3	89.8	90.0	90.6	90.1
aug-cc-pVDZ	88.7	89.4	89.8	90.4	89.8
cc-pVTZ	83.9	85.1	84.8	85.8	85.2
aug′-cc-pVTZ	82.9	84.1	83.9	84.5	84.0
observed[a]	85.07	84.30	87.00	86.37	

[a] One standard deviation uncertainties are: ±0.44, ±0.17, ±0.14, ±0.70, respectively.

Local Mode Calculations and Spectral Simulations. The CCSD(T) calculated local mode parameters for the OH-stretching vibrations of conformers **1**, **2**, and **3** are presented in Tables 4 and 5. The local mode parameters obtained with the cc-pVDZ basis set are surprisingly close to the observed values. The aug′-cc-pVDZ and aug-cc-pVDZ calculations underestimate the frequency $\tilde{\omega}$ by 20−30 cm^{-1} and overstimate the anharmonicity $\tilde{\omega}x$ by 3−5 cm^{-1}. The difference between the aug′-cc-pVDZ and aug-cc-pVDZ results is small, which supports our use of the approach of only adding diffuse functions on the hydroxyl groups. With the cc-pVTZ basis set, $\tilde{\omega}$ is overestimated by 10−20 cm^{-1} and $\tilde{\omega}x$ is in good agreement with observation. Frequencies obtained with the aug′-cc-pVTZ basis set were consistently in excellent agreement with observation with the largest deviation being 4 cm^{-1}. This is obtained without any scaling. The anharmonicities were 2−3 cm^{-1} too low with the exception of the **1**f transition which was calculated to be within the experimental uncertainty. The calculated range of anharmonicities for the three conformers are within 2 cm^{-1} of each other. Calculations using the CCSD(T)/cc-pVTZ method have previously been reported for fundamental frequencies to give an accuracy similar to that obtained in Table 4 for the OH-stretching local mode frequencies.[66,67]

We have calculated the normal-mode frequencies of conformer **1** with the CCSD(T)/aug-cc-pVDZ method in the ACES II program.[68] The OH_b- and OH_f-stretching harmonic frequencies are 3782 and 3830 cm^{-1}, respectively, and are in excellent agreement with the local mode frequencies we have reported in Table 4 for the same basis set. This supports our modeling of the OH-stretching vibrations as isolated local modes.

Table 6. Anharmonic Oscillator Calculated OH-stretching Wavenumbers (cm^{-1}) and Oscillator Strengths of Ethylene Glycol[a]

	1b		**1**f		
v	$\tilde{\nu}$	f_b	$\tilde{\nu}$	f_f	f_b/f_f
1	3640	5.4×10^{-6}	3688	4.4×10^{-6}	1.2
2	7115	3.9×10^{-7}	7207	6.3×10^{-7}	0.62
3	10423	1.5×10^{-8}	10559	2.3×10^{-8}	0.65
4	13566	8.1×10^{-10}	13742	1.1×10^{-9}	0.74
5	16543	7.4×10^{-11}	16757	7.9×10^{-11}	0.94
	2b		**2**f		
v	$\tilde{\nu}$	f_b	$\tilde{\nu}$	f_f	f_b/f_f
1	3624	5.9×10^{-6}	3654	3.3×10^{-6}	1.8
2	7080	3.8×10^{-7}	7185	5.1×10^{-7}	0.74
3	10368	1.5×10^{-8}	10454	2.0×10^{-8}	0.75
4	13488	8.5×10^{-10}	13600	9.5×10^{-10}	0.89
5	16441	7.9×10^{-11}	16578	7.5×10^{-11}	1.1
	3				
v	$\tilde{\nu}$	f^b			
1	3669	3.7×10^{-6}			
2	7169	4.6×10^{-7}			
3	10502	1.7×10^{-8}			
4	13666	8.2×10^{-10}			
5	16663	6.8×10^{-11}			

[a] Calculated with CCSD(T)/aug'-cc-pVTZ ab initio local mode parameters. [b] Intensity of a single OH oscillator. The values should be doubled for spectral comparison.

As shown in Figure 1, the OH bonds in conformer 3 have the same orientation (g^-) as the OH_b bonds in conformers **1** and **2**. If we compare the calculated local mode frequencies in Table 4, we see that the **1**b and **2**b frequencies are significantly lower than that of **3**. These redshifts of 30 and 45 cm^{-1} for **1** and **2**, respectively, are an indication of weak hydrogen bonding. It appears that **2** has slightly stronger intramolecular hydrogen bonding than **1**. However, both are weak compared to, e.g., water dimer, where the wavenumber redshift is approximately 100 cm^{-1}.[53] The anharmonic oscillator calculated wavenumbers and oscillator strengths of the OH-stretching transitions obtained at the CCSD(T)/aug′-cc-pVTZ level are presented in Table 6. The calculated ratio of the OH_b to OH_f oscillator strengths f_b/f_f are included. The intensity trend of hydrogen bonding, stronger f_b for the fundamental and weaker f_b for the first overtone compared to f_f, was calculated for both **1** and **2**. In the fundamental, the calculated intensity for **2**b is slightly larger than **1**b, whereas in the first overtone **2**b is marginally weaker than **1**b. This intensity trend would suggest that the intramolecular hydrogen bond interaction is slightly stronger in conformer **2**, and is in agreement with the **2**b transition having lower frequency than **1**b. With increasing overtone, f_b is calculated to steadily regain intensity relative to f_f for both **1** and **2**. Accurate intensities are difficult to obtain from the observed overtone spectra due to the overlap of the bands. However, **1**b appears to be slightly weaker than **1**f in all overtones, in good agreement with the calculated intensity ratios. For **2** similar ratios were predicted by our calculations, however in the spectra **2**b appears even weaker. From the relative abundances in Table 1 and the calculated intensities in Table 6, we would expect the OH-stretching transitions of **1** to appear

(66) Lee, T. J.; Martin, J. M. L.; Taylor, P. R. *J. Chem. Phys.* **1995**, *102*, 254−261.
(67) Martin, J. M. L.; Taylor, P. R. *Spectrochim. Acta Part A* **1997**, *53*, 1039−1050.
(68) Stanton, J. F.; et al. ACES II; Quantum Theory Project, University of Florida.

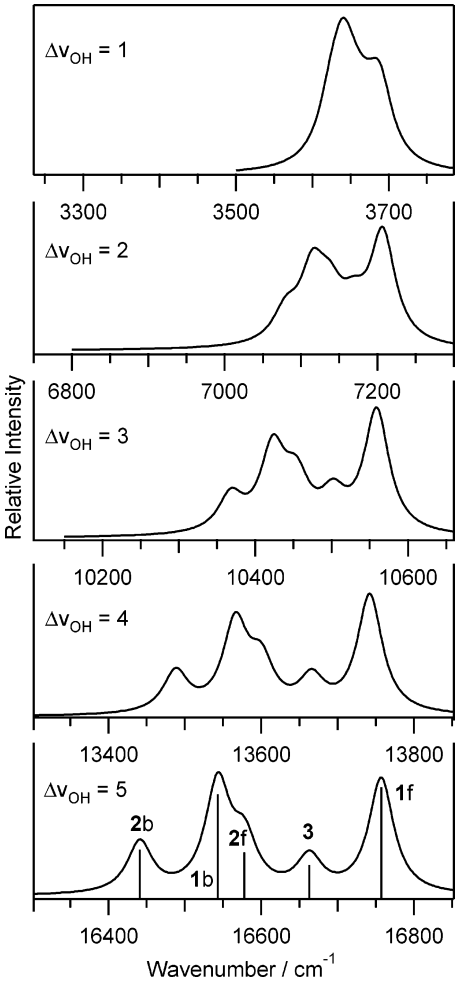

Figure 4. Simulated OH-stretching overtone spectra of ethylene glycol at 298 K based on the transitions presented in Table 6. A labeled stick spectrum is used to illustrate the transitions in the $\Delta v_{OH} = 5$ region. The abscissa of each spectral region is 550 cm^{-1} wide.

with approximately twice the intensity as the transitions of **2**, which is in good agreement with the observed spectra shown in Figure 3.

In Figure 4 we show the simulated spectra in the $\Delta v_{OH} = 1-5$ regions. The simulations are based on anharmonic oscillator local mode calculations with the CCSD(T)/aug′-cc-pVTZ ab initio parameters. Each transition was assigned a 40 cm^{-1} wide Lorentzian band to comprise the band contour, and the intensity of each transition was adjusted according to the calculated conformer abundances from Table 1. The calculated fundamental spectrum has a profile of two broad peaks and is in excellent agreement with the observed spectrum of Buckley and Giguère.[19] The close overlap of the transitions in the fundamental makes identification of specific conformers difficult. The calculated $\Delta v_{OH} = 2$ region is in agreement with our observed spectrum shown in Figure 2. For the $\Delta v_{OH} = 3-5$ overtones the agreement is also good, although at the higher overtones small wavenumber differences in the local mode parameters, especially the anharmonicity, can lead to significant frequency changes. The $v^2 + v$ dependence of the vibrational energy on $\tilde{\omega}x$ means that a 3 cm^{-1} variation in the calculated anharmonicity leads to a 90 cm^{-1} shift at $\Delta v_{OH} = 5$. Apart from a slightly larger intensity of **1**b and **2**b, particularly in the $\Delta v_{OH} = 5$ region, the fully ab initio simulated spectra match the observed spectra.

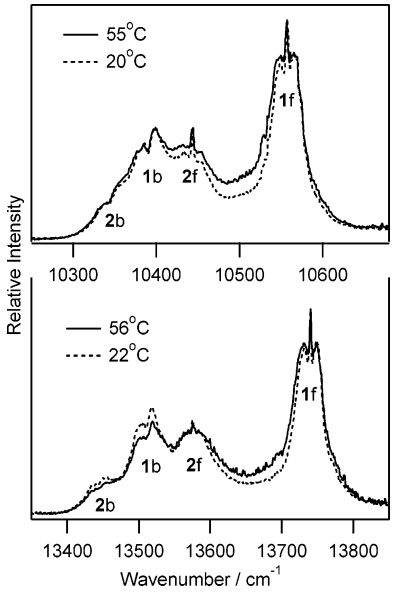

Figure 5. Variable temperature photoacoustic spectra of ethylene glycol vapor in the $\Delta v_{OH} = 3$ (top) and 4 regions. The spectra were scaled so that the height of the Q-branches of the **1**f transitions are equivalent.

Temperature Effects. The $\Delta v_{OH} = 3$ and 4 regions of EG were each recorded at different temperatures to observe the effects on the spectra. Conformers **1** (58%), **2** (26%) and **3** (10%) are calculated to comprise the bulk of the total population at room temperature. A temperature increase will increase the population of **2** and **3** relative to the most stable conformer **1**. The $\Delta v_{OH} = 3$ and 4 regions were recorded at room temperature and at approximately 55 °C and are shown in Figure 5. To simplify comparison, the spectra were scaled such that the height of the Q-branches of the **1**f transition within each overtone region are equivalent at each temperature. At a temperature of 55 °C the populations for **1**, **2**, and **3** are 54%, 26% and 11%, respectively.

Despite the small difference in the abundances, changes in the spectra are apparent which suggests the presence of **3**. In the $\Delta v_{OH} = 3$ and 4 spectra, we observe that the **2**f transition gains intensity relative to the **1**b transition with increasing temperature as expected from the increase in the abundance of **2**. An intensity increase around 10500 cm^{-1} in the $\Delta v_{OH} = 3$ region and 13 650 cm^{-1} in the $\Delta v_{OH} = 4$ region is also observed with higher temperature. These are the approximate positions where the OH-stretching transitions of **3** are expected. The differences in the spectra are subtle due to the overlap of the transitions and the moderate temperature used. Trace amount of H_2O vapor also contributes to the intensity around 13 650 cm^{-1}. A contribution from **3** is also observed in the spectrum of the $\Delta v_{OH} = 5$ region shown in Figure 3. The OH-stretching transitions of **3** appear as a high-energy shoulder on the **2**f transition slightly below 16 600 cm^{-1} in the spectrum of EG-d_4. This location is in agreement with our calculations. Thus evidence for conformer **3** is observed both in the temperature study and in the EG-d_4 spectrum.

Resonance Coupling. As mentioned, the EG and EG-d_4 spectra are virtually identical in the $\Delta v_{OH} = 3$ and 4 regions but differ significantly in the 16 400−16 600 cm^{-1} range in the $\Delta v_{OH} = 5$ region as shown in Figure 3. This observation strongly suggests resonance between pure OH-stretching states ($5v_{OH}$) and combination states involving both OH- and CH-stretching

modes ($4\nu_{OH} + \nu_{CH}$). Similar perturbations in this spectroscopic region have been observed in methanol[69] and formic acid,[42] where the "bright" $5\nu_{OH}$ state is in a strong resonance with the "dark" $4\nu_{OH} + \nu_{CH}$ combination state. The spectroscopic outcome of such a resonance is the borrowing of intensity from the bright state by the dark state and the splitting apart or "repulsion" of the frequencies of the two unperturbed states.[70] That such a strong resonance occurs is interesting as the OH and CH bonds are well separated.

The spectrum of EG-d_4 in the $\Delta\upsilon_{OH} = 5$ region is consistent with the lower overtones and is free from the perturbation observed for the EG spectrum. Thus a CH vibrational mode is involved in the perturbation. Two fundamental CH-stretching bands at 2941 and 2878 cm^{-1} have been observed in the vapor phase infrared spectrum of EG.[19] We have added these ν_{CH} frequencies to the observed $4\nu_{OH}$ frequencies to yield the approximate unperturbed $4\nu_{OH} + \nu_{CH}$ frequencies. The smallest absolute frequency differences calculated between these $4\nu_{OH} + \nu_{CH}$ frequencies and the unperturbed $5\nu_{OH}$ frequencies obtained from the EG-d_4 spectrum is small for **1**b (15 cm^{-1}), **2**b (16 cm^{-1}), and **2**f (27 cm^{-1}), making resonance coupling likely. In formic acid, the splitting between the $5\nu_{OH}$ and $4\nu_{OH}+\nu_{CH}$ states was 23 cm^{-1} and a strong resonance was observed in the overtone spectrum.[42] For the **1**f transition, the frequency difference is significantly larger at 70 cm^{-1} and there is little change in the **1**f transition between the EG and EG-d_4 spectra. In the lower overtones, these local mode combination states are too far away from the pure OH-stretching states for resonance to occur. For example, in the $\Delta\upsilon_{OH} = 4$ region, the $3\nu_{OH} + \nu_{CH}$ states are separated by more than 160 cm^{-1} from the $4\nu_{OH}$ states, and the EG and EG-d_4 spectra in Figure 3 look virtually identical.

In the $\Delta\upsilon_{OH} = 5$ spectra shown in Figure 3, the **1**b and **2**f transitions are clearly observed to be perturbed. The extra breadth in the region caused by the "repulsions" of the bright and dark states is a clear sign of this. The perturbed transitions produces what appears as three peaks in 16 400−16 600 cm^{-1} region of the EG spectrum, with a maximum near 16 500 cm^{-1}. The **2**b transition is weak and it is not as easy to observe if it has been perturbed.

In methanol and formic acid, the resonance occurs when the OH and CH bonds are trans to each other,[42,69] i.e., there is a 180° dihedral between the OH and CH bonds. The **1**b and **2**f bonds of EG are nearly trans in conformation with a CH bond, and thus it appears that this geometry facilitates this type of through-bond resonance.

Conclusions

The vapor phase OH-stretching overtone spectra of ethylene glycol and ethylene-d_4 glycol has been recorded in the $\Delta\upsilon_{OH} = 2-5$ regions to investigate the effects of weak intramolecular hydrogen bonds. Of the 10 unique conformers, the room-temperature spectra are dominated by two conformers, tG^+g^- and $g^+G^+g^-$, whose main geometrical difference is the dihedral angle of the "free" hydroxyl group. The vapor phase spectrum was also recorded at an elevated temperature in the $\Delta\upsilon_{OH} = 3$ and 4 regions. Evidence for the less abundant third conformer $g^-G^+g^-$ has been found in the temperature study as well as in the $\Delta\upsilon_{OH} = 5$ spectrum of ethylene-d_4 glycol. The relative abundances of the conformers were calculated at the B3LYP/aug-cc-pVTZ level.

High-level ab initio calculations with the CCSD(T)/aug′-cc-pVTZ method were performed to aid spectral interpretation. The OH-stretching local mode frequencies are in excellent agreement with observation. The local mode frequencies differ by less than 4 cm^{-1} and anharmonicities by less than 3 cm^{-1} for the four observed OH-stretching transitions. The OH-stretching transitions and intensities have been calculated with an anharmonic oscillator local mode model. The spectra have been simulated by taking into account the relative abundance of the conformers. The calculations have predicted the order of the OH-stretching transitions correctly. The calculated spacing between transitions differed from the observed values, owing to the 2−3 cm^{-1} difference between the calculated and observed anharmonicities. The calculated intensities are in good agreement with observation, and the CCSD(T)/aug′-cc-pVTZ method has proven successful in simulating overtone spectra without any empirical scaling.

Evidence for strong resonance coupling between OH and CH bonds has been found in ethylene glycol. The **2**f and **1**b OH-stretching transitions in the $\Delta\upsilon_{OH} = 5$ region are highly perturbed by resonance with the corresponding $4\nu_{OH} + \nu_{CH}$ states. This resonance phenomenon in the $\Delta\upsilon_{OH} = 5$ region is likely to be present in other molecules containing neighboring CH and OH moieties, particularly so if the CH and OH bonds are in a trans or nearly trans configuration.

Overtone spectroscopy in the gas phase is a powerful tool for observing weak intramolecular interactions. For the two lowest energy conformers, the characteristic redshift of the OH bonds involved in hydrogen bonding was observed. The intensity increase in the fundamental and subsequent decrease in the first overtone was determined from the anharmonic oscillator calculations. Interestingly, based on the magnitudes of these two properties, in addition to the CCSD(T)/aug′-cc-pVTZ geometries, the intramolecular hydrogen bond appears to be marginally stronger in the second most energetically preferred conformer.

Acknowledgment. We acknowledge the Marsden Fund and the International Science and Technology (ISAT) Linkage fund administered by the Royal Society of New Zealand, the Danish Research Agency, and the Danish Center for Scientific Computing for support.

Supporting Information Available: Table 2 with cc-pVDZ, aug′-cc-pVDZ, aug-cc-pVDZ, cc-pVTZ, and aug′-cc-pVTZ basis sets. CCSD(T)/aug′-cc-pVTZ optimized geometries of conformers **1**, **2**, and **3** in z-matrix format. CCSD(T)/aug-cc-pVDZ calculated normal-mode frequencies and intensities of conformer **1**. Complete refs 59, 62, and 68. This material is available free of charge via the Internet at http://pubs.acs.org.

JA055827D

(69) Boyarkin, O. V.; Lubich, L.; Settle, R. D. F.; Perry, D. S.; Rizzo, T. R. *J. Chem. Phys.* **1997**, *107*, 8409−8422.
(70) Herzberg, G. *Molecular Spectra and Molecular Structure II. Infrared and Raman Spectra of Polyatomic Molecules*; D. Van Nostrand: Princeton, 1945.